Letter

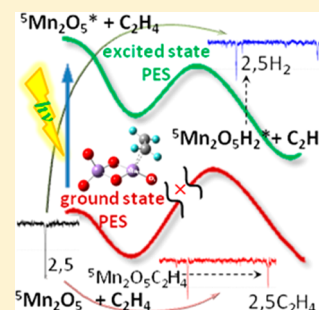# Ethylene C−H Bond Activation by Neutral Mn₂O₅ Clusters under Visible Light Irradiation

Shi Yin and Elliot R. Bernstein*

Department of Chemistry, NSF ERC for Extreme Ultraviolet Science and Technology, Colorado State University, Fort Collins, Colorado 80523, United States

Ⓢ Supporting Information

**ABSTRACT:** A photo excitation fast flow reactor coupled with a single-photon ionization (118 nm, 10.5 eV) time-of-flight mass spectrometry (TOFMS) instrument is used to investigate reactions of neutral $Mn_mO_n$ clusters with $C_2H_4$ under visible (532 nm) light irradiation. Association products $Mn_2O_5(C_2H_4)$ and $Mn_3O_{6,7}(C_2H_4)$ are observed without irradiation. Under light irradiation, the $Mn_2O_5(C_2H_4)$ TOFMS feature decreases, and a new species, $Mn_2O_5H_2$, is observed. This light-activated reaction suggests that the visible radiation can induce the chemistry, $Mn_2O_5 + C_2H_4 + h\nu_{(532\ nm)} \rightarrow Mn_2O_5^*(C_2H_4) \rightarrow Mn_2O_5H_2 + C_2H_2$. High barriers (0.67 and 0.59 eV) are obtained on the ground-state potential energy surface (PES); the reaction is barrierless and thermodynamically favorable on the first excited-state PES, as performed by time-dependent density functional theory calculations. The calculational and experimental results suggest that $Mn_2O_5$-like structures on manganese oxide surfaces are the appropriate active catalytic sites for visible light photocatalysis of ethylene dehydrogenation.

Interaction of the C−H bond of a small hydrocarbon molecule with a bare transition-metal neutral atom is the simplest model for one of the most fundamental and important catalytic steps in a wide range of catalytic reactions.[1,2] Gas-phase reactions of ethylene with bare transition-metal atoms, such as Y, Zr, and Nb, have been investigated through a number of experiments.[3,4] In these reactions, C−H bond activation products, including C−H insertion and H₂-elimination products, are found to be the common products. Ethylene reactions over different single-crystal metal surfaces are also widely studied;[5−11] the general goal of these studies is elucidation of the elementary reaction paths for ethylene dehydrogenation. An ideal approach for probing and understanding the "active sites" on the surface of a catalyst at a strictly molecular/atomic level is the study of "isolated" gas-phase clusters; such systems are generated in a nonperturbing environment; thus, their structure and activity can be readily identified both experimentally and theoretically.[12,13] Manganese oxides represent an interesting class of compounds with important technological applications[14] in catalysis.[15] Our recent attention toward manganese oxide clusters is due to the emerging use of manganese oxides in biomedical, photo-catalysis, and supercapacitor applications; this material is additionally relatively inexpensive, nontoxic, and naturally abundant.[16−20] Manganese oxide clusters have thereby been the subject of a limited number of theoretical and experimental investigations in recent years.[21−26] $Mn_2O_3$ is suggested to be a potential light-harvesting application material,[27] and successful application of manganese oxides to the photocatalytic degradation of various dyes[19,28] and textile manufacturing effluents[20,29] under visible light have been reported. The photoinduced reactions of gas-phase metal (gold and silver) clusters have also been reported recently.[30] To the best of our knowledge, however, the visible light photocatalytic reaction of gas-phase neutral manganese oxide species has not been reported.

To study the potential photocatalytic application of manganese oxide for C−H bond activation, and to understand the possible reaction mechanism at a molecular level, we present in this Letter the first study of visible light photocatalytic C−H bond activation of ethylene over neutral $Mn_2O_5$ clusters at room temperature. We employ a newly constructed photoexcitation fast flow reactor system coupled with single-photon ionization (SPI). This latter technique has proved to be reliable for detecting distributions and reactivities of neutral clusters without dissociation or fragmentation.[31−33] To demonstrate this reaction and determine its possible mechanisms, density functional theory (DFT) and time-dependent (TD-DFT) calculations are performed to investigate the activity of $Mn_mO_n$ clusters toward ethylene C−H bond activation on their ground- and first excited-state potential energy surfaces (PES). Active sites and details of the reaction mechanism are obtained; we propose related condensed phase, atomic/molecular level, and catalytic processes for dehydrogenation of ethylene over manganese oxide under visible light irradiation.

The experimental setup for laser ablation employed in this work has been described previously in detail.[34−37] A new photoexcitation fast flow reactor system is constructed to investigate reactions under visible light irradiation.[34] $Mn_mO_n$ clusters are generated in a laser ablation source; manganese
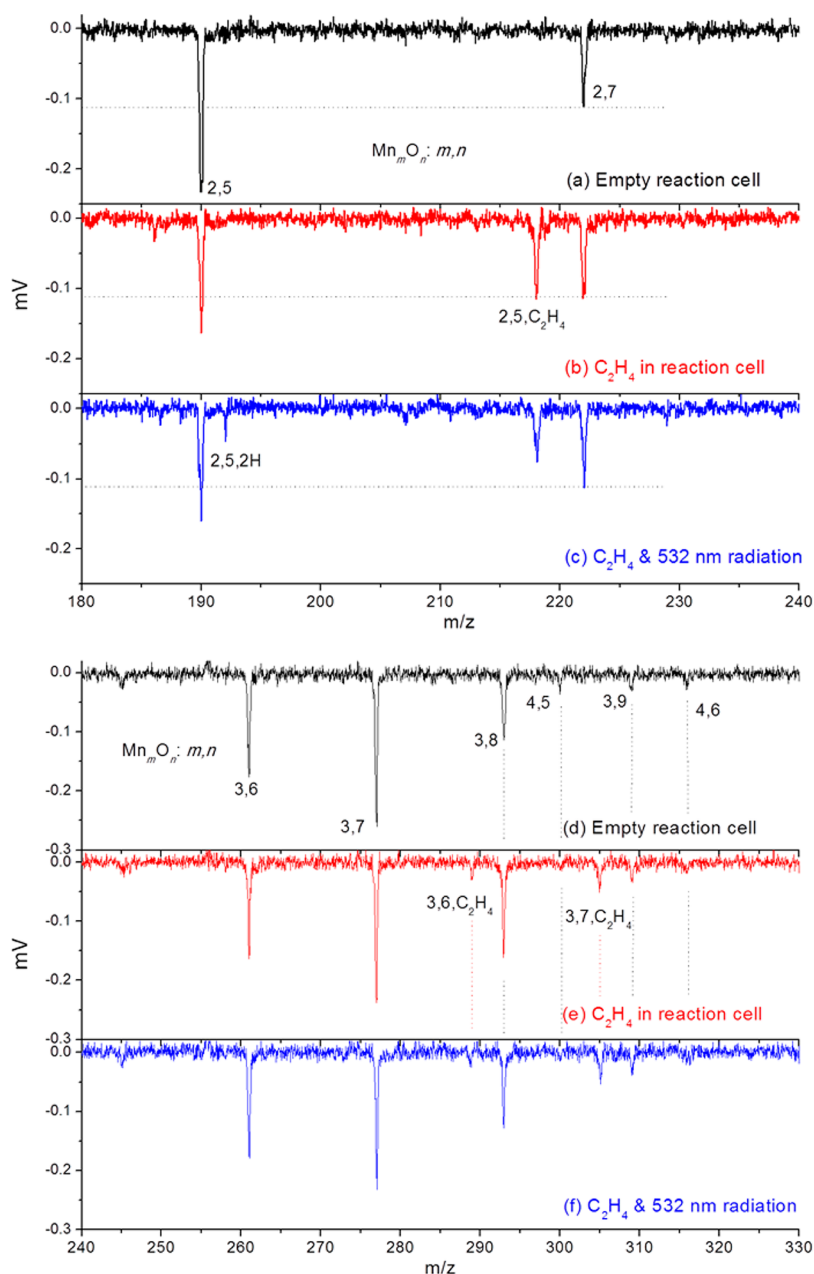
**Figure 1.** Reactions of neutral $Mn_mO_n$ clusters with $C_2H_4$ with and without 532 nm light irradiation: (a, d) no reaction gas, (b, e) $C_2H_4$, and (c, f) $C_2H_4$ with 532 nm radiation in a fast flow reactor. Products $Mn_mO_n(C_2H_4)_{0,1}$ are labeled as $m, n$ and $m, n, C_2H_4$, respectively. See text for details.

plasma, ablated from a manganese foil disk, reacts with oxygen seeded in the helium (5% $O_2$/He) expansion gas. The expansion gas is pulsed into the vacuum by a supersonic nozzle (R. M. Jordan, Co.) with a backing pressure of typically 75 psi. Generated $Mn_mO_n$ clusters react with reactant gas ($C_2H_4$) in a fast flow quartz reactor (i.d. 6.8 mm × 68 mm), which is directly coupled to the cluster generation channel (i.d. 1.8 mm × 19 mm). A 10 Hz, focused, 532 nm $Nd^{3+}$:YAG laser ($Nd^{3+}$ yttrium aluminum garnet) with ∼6 mJ/pulse energy is used for the laser ablation. The other 10 Hz, defocused, 532 nm $Nd^{3+}$:YAG laser with ∼25 mJ per pulse (∼5 mJ/cm²) energy is used for the laser light irradiation dispersed over the quartz reactor. The pressure in the fast flow reactor can be estimated ∼14 Torr for the reaction.[38] Reactants and products are thermalized to 300−400 K by collision during the reaction.[39] An electric field downstream of the reactor removes any

residual ions from the molecular beam. The beam of neutral reactants and products is skimmed into a differentially pumped chamber and ionized by a separated vacuum ultraviolet laser beam (118 nm, 10.5 eV/photon). After the near threshold ionization, photoions are detected by a time-of-flight mass spectrometer.

Calculations of the structural parameters for neutral $Mn_mO_n$ clusters and the reactions of $C_2H_4$ and $O_3$ with $Mn_2O_5$ (reactive) and $Mn_3O_7$ (unreactive) clusters are performed employing DFT. The hybrid B3LYP exchange−correlation functional[40−42] and a 6-311+G(d) basis set[43−45] are used. Choice of the B3LYP/6-311+G(d) method with moderate computational cost has been tested to provide reasonable results in previous studies on manganese oxide clusters;[22−24] this approach yields good results for the interpretation of vibrational spectra of manganese oxides.[21,46] Binding energies
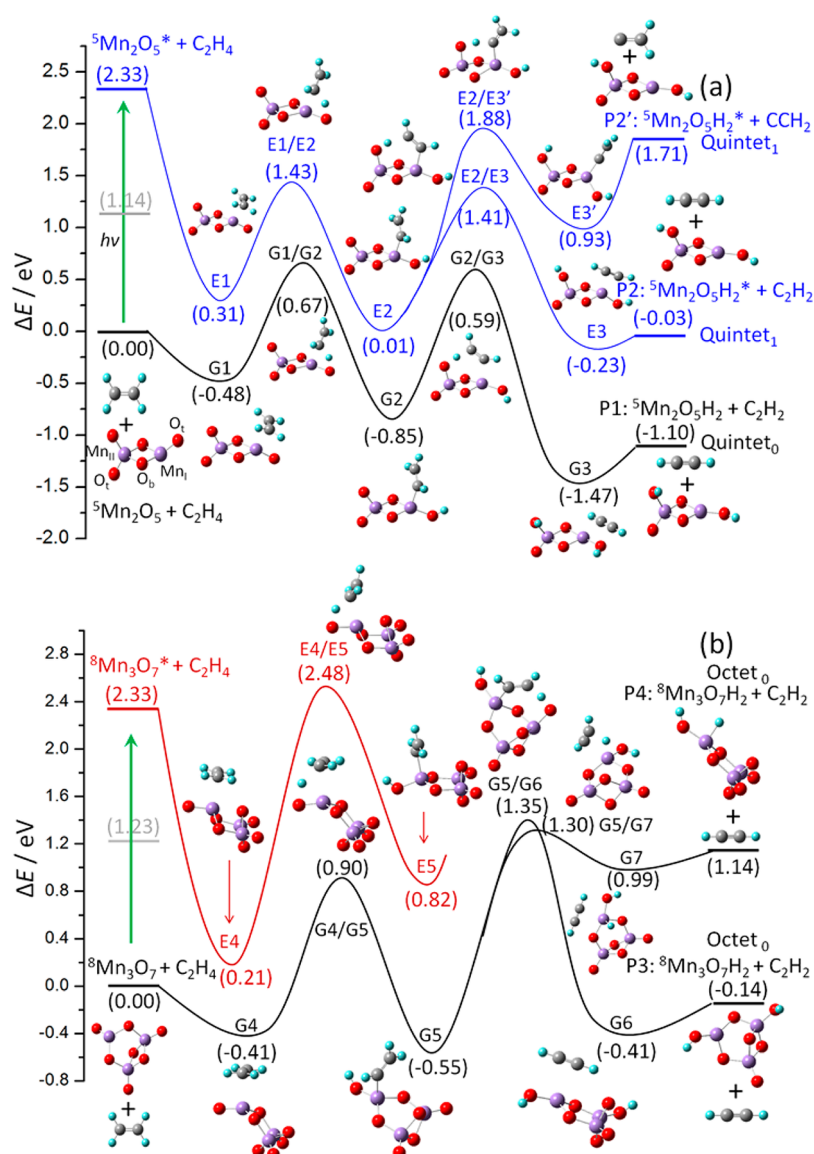
**Figure 2.** Potential energy surface profiles of ground and excited states for reactions (a) $Mn_2O_5 + C_2H_4 \rightarrow Mn_2O_5H_2 + C_2H_2$ and (b) $Mn_3O_7 + C_2H_4 \rightarrow Mn_3O_7H_2 + C_2H_2$. Energies are in electronvolts and relative to the initial reactant energy of $^5Mn_2O_5 + C_2H_4$, and $^8Mn_3O_7 + C_2H_4$, respectively. Energy levels are calculated at the B3LYP/6-311+G(d) level. The spin multiplicity ($M$) is listed as $^MMn_mO_n$. See text for details.

between neutral $Mn_mO_n$ and reactants are calculated at different typical association geometries to obtain the lowest-energy structures. DFT and TD-DFT calculations are performed to explore the ground- and first excited-state PESs for the reactions $Mn_2O_5/Mn_3O_7 + C_2H_4 \rightarrow Mn_2O_5H_2/Mn_3O_7H_2 + C_2H_2$, involving geometry optimizations of the reactants, intermediates, transition states, and products. Vibrational frequency calculations are further performed to confirm the global minima and transition states, which have zero and one imaginary frequency, respectively. The relative energies (given in electronvotls) are corrected for zero point energy (ZPE) contributions. Additionally, intrinsic reaction coordinate (IRC) calculations are carried out to determine if an estimated transition state connects two appropriate local minima along the reaction pathway. Binding energies are calculated for a few species employing the basis set superposition error (BSSE) counterpoise correction;[47,48] these corrections are found to be insignificant at the present level of theory. Reaction

mechanisms for the observed chemical reactions are determined employing the above procedures.

Figure 1a shows the distribution of neutral manganese oxide clusters within the mass range of $m/z = 180-240$. The $Mn_mO_{2m}$ and $Mn_mO_{2m+1}$ series are found to be the most stable neutral cluster species for $O_2$ concentrations in the range 1–10% in the expansion gas.[24] Mass spectra generated from the reaction of $Mn_2O_5$ clusters with $C_2H_4$ are presented in Figure 1b. Association product $Mn_2O_5C_2H_4$ is observed for $C_2H_4$ used as the reactant gas, indicating $Mn_2O_5$ clusters are able to adsorb single molecules of $C_2H_4$. The calculation result suggests the binding energy ($E_b$) of $Mn_2O_5$ with $C_2H_4$ is 0.48 eV, which is smaller than the binding energy of $C_2H_4$ with some bare metal atoms (Pd, 1.30 eV; Nb, 0.79 eV; and Pt, 0.74 eV).[49,50] Under 532 nm laser light irradiation, the signal intensity of $Mn_2O_5(C_2H_4)$ decreases to about one-half of its original (no radiation) value (see Figure 1c), while a new mass peak $Mn_2O_5H_2$ is observed. The intensity of $Mn_2O_5H_2$ does not increase when the light irradiation laser energy is higher than 25

mJ per pulse. This experiment result suggests the likely reaction, $Mn_2O_5 + C_2H_4 + hv_{(532\ nm)} \rightarrow Mn_2O_5H_2 + C_2H_2$.

The potential energy surface of ground ($Q_0$) and first quintet excited states ($Q_1$) for the reaction $Mn_2O_5 + C_2H_4 \rightarrow Mn_2O_5H_2 + C_2H_2$ are studied at the B3LYP/6-311+G(d) level by DFT and TD-DFT calculations (Figure 2a), respectively. The $Mn_2O_5$ cluster contains two bridge-bonded oxygen ($O_b$), three terminally bonded oxygen ($O_t$), and two manganese atoms. $Mn_I$ bonds to one $O_t$ atom, and $Mn_{II}$ bonds to two $O_t$ atoms. On the $Q_0$ potential energy surface (shown in Figure 2a, black line), the reaction starts with an exothermic addition of $C_2H_4$ to $Mn_I$ of quintet $Mn_2O_5$ to form a stable complex, $Mn_2O_5(C_2H_4)$ (intermediate G1) with 0.48 eV adsorption energy. Two H atoms transfer from $C_2H_4$ to $O_t$ atoms on $Mn_I$ and $Mn_{II}$ step by step (through transition states G1/G2 and G2/G3), leading to the formation of an OH moiety on each Mn center (intermediate G3). The $Q_0$ PES possesses a significantly high overall reaction barrier (ORB, 0.67 eV) for the reaction. This ORB is determined for the transformation of intermediate G1 to intermediate G2 through transition state G1/G2, during which step the first H atom from $C_2H_4$ transfers to $Mn_2O_5$. Evaporation of the $C_2H_2$ moiety from intermediate G3 leads to the formation of products $Mn_2O_5H_2 + C_2H_2$ (P1), whose energy is 1.1 eV lower than that of the reactants $Mn_2O_5 + C_2H_4$ of the entrance channel. The positive high ORB (0.67 eV) indicates that the reaction ($Mn_2O_5 + C_2H_4 \rightarrow Mn_2O_5H_2 + C_2H_2$) cannot occur on the ground-state PES at room temperature. This calculational result is in good agreement with the experimental observation presented in Figure 1b: without 532 nm irradiation of the reactants, only a stable association product $Mn_2O_5C_2H_4$ is observed.

The $Q_0 - Q_1$ vertical excitation energy of $Mn_2O_5$ (1.14 eV, as calculated by TD-DFT) is lower than the 532 nm photon energy (2.33 eV), which suggests the ground-state $Mn_2O_5$ can absorb a 532 nm photon and be excited to its first quintet excited state. On the first excited-state ($Q_1$) PES, reaction is found to be thermodynamically favorable (−2.36 and −0.62 eV) for generation of excited-state products P2 and P2′, as shown in Figure 2a (blue line). This result suggests a reasonable mechanism for the observed light irradiation experimental spectra shown in Figure 1c. When 532 nm laser light irradiates the fast flow reactor, the signal intensity of $Mn_2O_5(C_2H_4)$ decreases, and a new mass peak $Mn_2O_5H_2$ appears. A possible reaction mechanism for this dehydrogenation of ethylene on $Mn_2O_5$ clusters under light irradiation is that the $Mn_2O_5$ cluster is excited ($Q_1 \leftarrow Q_0$) and then takes H atoms from the $C_2H_4$ one by one (from intermediate E1 to intermediate E3 through transition states E1/E2 and E2/E3, or from intermediate E1 to intermediate E3′ through transition states E1/E2 and E2/E3′, respectively). Because the energy of transition state E2/E3′ is 0.47 eV higher than that of transition state E2/E3, and the energy of products P2′ ($Mn_2O_5H_2$ and vinylidene) is 1.74 eV higher than that of products P2 ($Mn_2O_5H_2$ and acetylene), the main products should be $Mn_2O_5H_2$ and acetylene (products P2) on the first excited-state PES. $Mn_I$ atoms of reactive $Mn_2O_5^*$ clusters (excited by 532 nm light) are the active sites for holding $C_2H_4$ molecules during the H transferring processes, and both the terminal oxygen atoms on $Mn_I$ and $Mn_{II}$ are the active ones for $C_2H_4$ dehydrogenation.

Additionally, the $Q_0 - Q_1$ vertical excitation energy of $Mn_2O_5C_2H_4$ (intermediate G1) is calculated to be 0.88 eV by TD-DFT (also lower than the 532 nm photon energy, 2.33

eV). This suggests that the ground-state association product $Mn_2O_5C_2H_4$ is also able to absorb a 532 nm photon and be excited to its first excited state. Thus, another possible reaction mechanism for the $C_2H_4$ dehydrogenation on $Mn_2O_5$ under visible light irradiation can be proposed: a $Mn_2O_5$ cluster adsorbs a $C_2H_4$ molecule, and the association product $Mn_2O_5C_2H_4$ is excited by 532 nm radiation; the 2.33 eV (adsorbed photon energy) excess energy in the excited $Mn_2O_5C_2H_4^*$ is sufficient to overcome reaction barriers on the first excited-state ($Q_1$) PES. Products $Mn_2O_5H_2^* + C_2H_2$ (P2) then are formed, following the reaction path shown in Figure 2a.

Other possible mechanisms (reaction coordinates) may also exist for the reaction $Mn_2O_5 + C_2H_4 \rightarrow Mn_2O_5H_2 + C_2H_2$, under visible light irradiation. For example, both the reaction of excited $Mn_2O_5^*$ (absorbing a 532 nm photon) with $C_2H_4$ and the reaction of excited association product $Mn_2O_5C_2H_4^*$ (absorbing a 532 nm photon) are possible reaction channels by which to generate products $Mn_2O_5H_2$ and $C_2H_2$ on the ground-state PES ($Q_0$) through conical intersections between the first excited- and ground-state potential energy surfaces. The latter possibility would be similar to the published (essential) mechanism for $H_2O$ oxidation by neutral $Ti_2O_5$ clusters under visible light irradiation.[34] Due to the possibility of collisional cooling in the reaction cell, not all excited-state clusters $Mn_2O_5C_2H_4^*$ must generate products $Mn_2O_5H_2$ and $C_2H_2$. Under these conditions, $Mn_2O_5$ and $C_2H_4$ or $Mn_2O_5C_2H_4$ are both potential nonreactive outcomes. The real reaction is a complex process. Only the one possible mechanism is discussed here in detail, as shown in Figure 2a. The point is that the dehydrogenation of $C_2H_4$ on $Mn_2O_5$ clusters ($Mn_2O_5 + C_2H_4 \rightarrow Mn_2O_5H_2 + C_2H_2$) cannot occur on the ground-state PES at room temperature, but the dehydrogenation is favorable through the first excited-state PES under visible light irradiation (532 nm). In other words, $Mn_2O_5$ is a size-dependent photocatalytic manganese oxide cluster site for the $C_2H_4$ dehydrogenation under visible light irradiation.

Both $Mn_2O_5$ and $Mn_3O_7$ clusters have high reactivity for CO oxidation,[24] so the $Mn_3O_7$ is selected as a comparison species to study the photocatalytic reactivity of other manganese oxide clusters. Association products $Mn_3O_6(C_2H_4)$ and $Mn_3O_7(C_2H_4)$ are observed (Figure 1e). The experimental results presented in Figure 1f demonstrate that the association products $Mn_3O_6(C_2H_4)$ and $Mn_3O_7(C_2H_4)$ do not change under the visible light irradiation. To understand why these latter clusters are not photocatalytically active, the PESs of the ground ($O_0$) and first excited ($O_1$) octet states are calculated for the reaction $Mn_3O_7 + C_2H_4 \rightarrow Mn_3O_7H_2 + C_2H_2$ and are presented in Figure 2b. On the ground-state PES, significant ORB of 0.90 eV (transition state G4/G5) and 1.35 eV (transition state G5/G6) and 1.30 eV (transition state G5/G7) are determined for the reaction paths to produce P3 and P4, respectively. The $O_0 - O_1$ vertical excitation energy of $Mn_3O_7$ (1.23 eV), as calculated by TD-DFT, is lower than the 532 nm photon energy (2.33 eV). The calculated absorption range (blue line) for $Mn_3O_7$ cluster is from about 350 nm (3.5 eV) to 1000 nm (1.2 eV), and for the $Mn_2O_5$ cluster is from about 400 nm (3.1 eV) to 900 nm (1.4 eV) (see calculated optical absorption of $Mn_2O_5$ and $Mn_3O_7$ clusters, Figure S1 in Supporting Information). These results suggest that both $Mn_2O_5$ and $Mn_3O_7$ clusters can be excited by absorbing 532 nm visible light. A high ORB of transition state E4/E5 (2.48

eV), however, is obtained for the first H atom transferring from $C_2H_4$ to the terminal O of $Mn_3O_7$ on the $O_1$ state PES (Figure 2b, red line). High positive ORBs on both $O_0$ and $O_1$ PESs for the reaction $Mn_3O_7 + C_2H_4 \rightarrow Mn_3O_7H_2 + C_2H_2$, suggest the $Mn_3O_7$ is nonreactive with $C_2H_4$ even under 532 nm visible light irradiation.

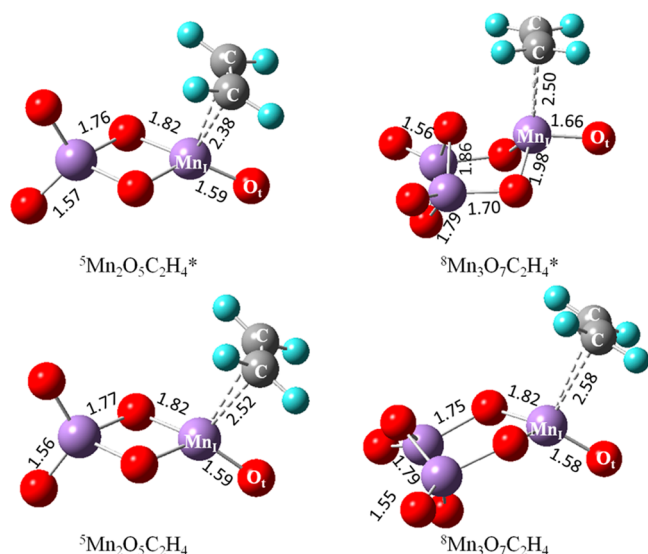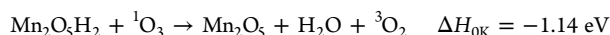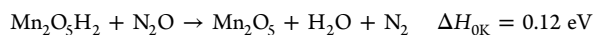According to the calculated lowest-energy geometry of $C_2H_4$ association products with $Mn_2O_5$ and $Mn_3O_7$ (Figure 3), two
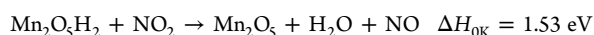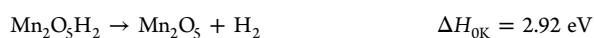


**Figure 3.** DFT optimized structures for ground- and first excited-state $Mn_2O_5(C_2H_4)$ and $Mn_3O_7(C_2H_4)$. For each cluster, the lowest-energy structure with bond lengths (in angstroms) and spin multiplicity ($M$: $^MMn_mO_n$) are listed.
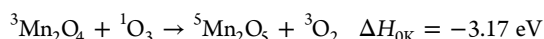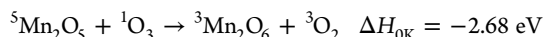
carbon atoms of $C_2H_4$ connect with $Mn_I$ atom of $Mn_2O_5$ and $Mn_3O_7$ through ethylene $\pi$-orbitals. The theoretically derived structure of these mixed organic/inorganic clusters have the following characteristics: the $Mn_IC$ bond length (2.38 Å) for excited-state $^5Mn_2O_5C_2H_4^*$ is 0.14 Å shorter than that (2.52 Å) of ground-state $^5Mn_2O_5C_2H_4$; the terminal $Mn_IO_t$ bond length (1.59 Å) of excited-state $^5Mn_2O_5(C_2H_4)^*$ is the same as that of ground-state $^5Mn_2O_5C_2H_4$; the $Mn_IC$ bond length (2.50 Å) of excited-state $^8Mn_3O_7(C_2H_4)^*$ is 0.08 Å shorter than that of ground-state $^8Mn_3O_7(C_2H_4)$ (2.58 Å); and the terminal $Mn_IO_t$ bond length (1.66 Å) of excited-state $^8Mn_3O_7(C_2H_4)^*$ is 0.08 Å longer than that (1.58 Å) of ground-state $^8Mn_3O_7(C_2H_4)$. The longer $Mn_IC$ and terminal $Mn_IO_t$ bond lengths of $^8Mn_3O_7C_2H_4^*$, compared to that of $^5Mn_2O_5C_2H_4^*$, are possible reasons for the high ORB of the first H atom transfer from $C_2H_4$ to $O_t$ on $Mn_I$ of $^8Mn_3O_7C_2H_4^*$ (transition state **E4/E5**, 2.48 eV shown in Figure 2b). Recall that the ORB for $^5Mn_2O_5C_2H_4^*$ (transition state **E1/E2**) is ~1.43 eV (Figure 2a). The highest occupied molecular orbitals (HOMOs), which are singly occupied, and the lowest unoccupied molecular orbitals (LUMOs) for ground-state $^5Mn_2O_5$ and $^8Mn_3O_7$ neutral clusters are also studied (shown in Figure S2). The HOMOs for $^5Mn_2O_5$ and $^8Mn_3O_7$ are composed of nonbonding d atomic orbitals of $Mn_I$ (IV, oxidation state) and their bonded $O_t$ p atomic orbitals, and the LUMOs, which are localized on the other Mn atoms, are also composed of nonbonding d atomic orbitals of Mn and p atomic orbitals of their bonded $O_t$ atoms. This molecular orbital description suggests that the ground to first excited-state excitations of both

$^5Mn_2O_5$ and $^8Mn_3O_7$ arise from a similar change in electron densities. The $Mn_I$ atoms in both clusters have oxidation states of IV, the Mn atom in $^5Mn_2O_5$ has an oxidation state of VI, and each of the two Mn atoms of $^8Mn_3O_7$ has an oxidation state of V, as indicated in Figure S2. These similar HOMO (singly occupied) and LUMO distribution characteristics for $^5Mn_2O_5$ and $^8Mn_3O_7$ are likely reasons for their similar vertical excitation energies ($Mn_2O_5$, 1.14 eV; $Mn_3O_7$, 1.23 eV). Nonetheless, this orbital similarity does not account for their different reactivities toward ethylene.

For a practical photocatalytic dehydrogenation of ethylene, the catalyst must be recycled. To generate a complete catalytic cycle for ethylene dehydrogenation on manganese oxide clusters, different $Mn_2O_5$ regenerative reactions from $Mn_2O_5H_2$ to $Mn_2O_5$ are calculated to explore the potential regeneration of the photocatalytically active manganese oxide cluster ($Mn_2O_5$):

$$Mn_2O_5H_2 \rightarrow Mn_2O_5 + H_2 \qquad \Delta H_{0K} = 2.92 \text{ eV}$$

$$Mn_2O_5H_2 + NO_2 \rightarrow Mn_2O_5 + H_2O + NO \quad \Delta H_{0K} = 1.53 \text{ eV}$$

$$Mn_2O_5H_2 + N_2O \rightarrow Mn_2O_5 + H_2O + N_2 \quad \Delta H_{0K} = 0.12 \text{ eV}$$

$$Mn_2O_5H_2 + {}^1O_3 \rightarrow Mn_2O_5 + H_2O + {}^3O_2 \quad \Delta H_{0K} = -1.14 \text{ eV}$$

As the first step of the potential energy profile shown in Figure S3, the reaction of $Mn_2O_5H_2$ with singlet and triplet $O_3$ to generate $Mn_2O_6H_2 + O_2$ is a barrierless process. After that, the calculational results show that no positive ORBs (only negative ORBs of $-1.31$ and $-1.36$ eV, referenced to the initial reactants $^5Mn_2O_5H_2 + {}^1O_3$) exist for the dehydrogenation of $Mn_2O_5H_2$. The crossing of spin triplet and singlet potential energy surfaces (spin conversion[51]) is obtained; this surface crossing suggests that both initial reactants $^5Mn_2O_5H_2 + {}^1O_3$ and $^5Mn_2O_5H_2 + {}^3O_3$ can form products $^5Mn_2O_5 + H_2O + {}^3O_2$ through the spin conversion point. These calculation results imply that ozone is a possible oxidant for regeneration of the photocatalytically reactive $Mn_2O_5$ clusters for ethylene dehydrogenation. Reactions of ozone with some initial manganese oxide clusters, such as $Mn_2O_4$ and $Mn_2O_5$, are also calculated.

$$^5Mn_2O_5 + {}^1O_3 \rightarrow {}^3Mn_2O_6 + {}^3O_2 \quad \Delta H_{0K} = -2.68 \text{ eV}$$

$$^3Mn_2O_4 + {}^1O_3 \rightarrow {}^5Mn_2O_5 + {}^3O_2 \quad \Delta H_{0K} = -3.17 \text{ eV}$$

These results suggest $Mn_2O_4$ and $Mn_2O_5$ are possibly oxidized by ozone; therefore, during the process of regeneration of the photocatalytically reactive $Mn_2O_5$ from $Mn_2O_5H_2$ by ozone, the generation of $Mn_2O_{5,6}$ from $Mn_2O_{4,5}$ oxidized by ozone must be considered carefully in practical catalytic processes.

Reactive clusters in the gas phase can be seen as a good model system for the active moieties (possibly defects) that exist on a catalyst surface. Thereby, a catalytic reaction of ethylene dehydrogenation and $Mn_2O_5$ moiety regeneration by $O_3$ on manganese oxide surfaces are proposed and presented schematically in Figure 4. This proposal is offered based on experimental and calculational results presented in Figures 1, 2, and S3. Our proposed mechanism indicates that the $C_2H_4$ molecule adsorbs on the $Mn_I$ site of the $Mn_2O_5$ moiety, which binds to only one terminal oxygen atom, and H atoms transfer to the active $O_t$ atoms on $Mn_I$ and the adjacent $Mn_{II}$ site step by step under visible light irradiation. $C_2H_2$ molecules can be formed and desorbed leaving $Mn_I$ sites on a catalytic
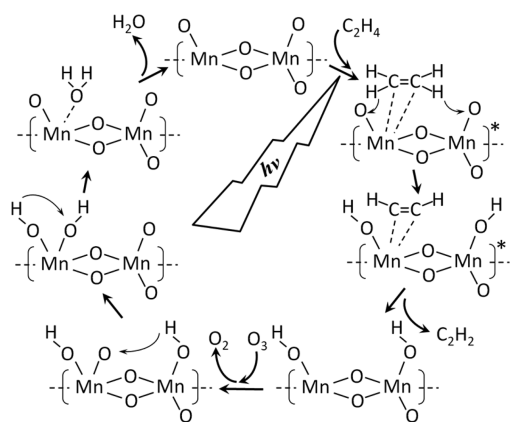
**Figure 4.** Possible photocatalytic cycle for ethylene oxidation by $O_3$ over manganese oxide catalysts at a molecular level.

manganese oxide surface. Ozone is selected here as a possible oxidant for regeneration of the $Mn_2O_5$ moiety. $O_3$ molecules can oxidize the $Mn_I$ sites to generate HO-$Mn_I$-O sites. $H_2O$ molecules are formed through H transfers and desorbed, leaving the photocatalytic manganese oxide surface unchanged. Ethylene dehydrogenation is thereby possible over the manganese oxide catalyst surface under visible light irradiation, and the catalyst surface can be regenerated and reactivated by ozone. Note that ozone is able to react with ethylene to form an ozonide to then cleave the C=C bond of ethylene;[52] therefore, ozone is only a possible (not the best and ideal) oxidant selected to reactivate the manganese oxide catalyst surface. The catalytic process (schematically depicted in Figure 4) is helpful for the understanding of the heterogeneous photocatalytic reaction mechanism of ethylene dehydrogenation on condensed-phase catalyst surfaces; this catalyst regeneration reaction is best performed in the absence of both $C_2H_4$ and $C_2H_2$.

In summary, reactions of neutral $Mn_mO_n$ ($m$ = 2, $n$ = 5, 7; $m$ = 3, $n$ = 6−8) clusters with $C_2H_4$ under visible (532 nm) light irradiation are investigated employing a photoexcited fast flow reactor system. Association products $Mn_2O_5(C_2H_4)$ and $Mn_3O_{6,7}(C_2H_4)$ are observed for reactions of $C_2H_4$ without light irradiation. With 532 nm laser light irradiation, the $Mn_2O_5(C_2H_4)$ feature decreases in intensity, and a new product $Mn_2O_5H_2$ is observed. This activation suggests that visible (532 nm) light radiation can induce chemistry for $Mn_2O_5$ with $C_2H_4$: $Mn_2O_5 + C_2H_4 + hv_{(532 \ nm)} \rightarrow Mn_2O_5*C_2H_4 \rightarrow Mn_2O_5H_2 + C_2H_2$. DFT and TD-DFT calculations are performed to explore the ground- and first excited-state PESs for the reactions $Mn_2O_5/Mn_3O_7 + C_2H_4 \rightarrow Mn_2O_5H_2/Mn_3O_7H_2 + C_2H_2$ and derive mechanisms for the reactions. High barriers (0.67 and 0.59 eV) are obtained on the ground-state PES for the $Mn_2O_5 + C_2H_4$ reaction, while the reaction is thermodynamically favorable on the first excited-state PES. The $Mn_I$ atoms of reactive (catalytic) $Mn_2O_5$ clusters are the active sites for holding $C_2H_4$ molecules during the $C_2H_4$ dehydrogenation processes under visible light (532 nm) irradiation. The next essential step is the first H atom transfer to the terminal $O_t$ on $Mn_I$; this H atom transfer has the highest barrier on the excited-state PES. The ORB of this first H atom transfer step appears to be an important factor with regard to $Mn_mO_n$ cluster photoreactivity with $C_2H_4$ and is suggested to be related to bond lengths of $Mn_IC$ and $Mn_IO_t$. The reaction mechanisms explored by calculations are in good agreement with the

experimental results and suggest that $Mn_2O_5$ moieties on a manganese oxide surface are active catalytic sites for visible light photocatalysis of $C_2H_4$.

## ■ ASSOCIATED CONTENT

**Ⓢ Supporting Information**

The Supporting Information is available free of charge on the ACS Publications website at DOI: 10.1021/acs.jpclett.6b00541.

> Optical spectra of $Mn_2O_5$ and $Mn_3O_7$ clusters using TDDFT calculations; DFT orbital plots showing the HOMO and LUMO of neutral $Mn_2O_5$ and $Mn_3O_7$ clusters; and potential energy surface profile of ground-state reaction $Mn_2O_5H_2 + O_3$ (PDF)

## ■ AUTHOR INFORMATION

**Corresponding Author**
*E-mail: erb@lamar.colostate.edu.

**Notes**
The authors declare no competing financial interest.

## ■ REFERENCES

(1) Koppen, P. A. M.; Kemper, P. R.; Bowers, M. T.; Freiser, B. S. *Organometallic Ion Chemistry*; Kluwer: Dordrecht, The Netherlands, 1996.

(2) Davies, J. A.; Watson, P. L.; Greenberg, A.; Liebman, J. F. *Selective Hydrocarbon Activation: Principles and Progress*; VCH: New York, 1990.

(3) Willis, P. A.; Stauffer, H. U.; Hinrichs, R. Z.; Davis, H. F. Reaction Dynamics of Zr and Nb with Ethylene. *J. Phys. Chem. A* **1999**, *103*, 3706−3720.

(4) Porembski, M.; Weisshaar, J. C. Kinetics and Mechanism of the Reactions of Ground-State Y ($4d^15s^2$, $^2D$) with Ethylene and Propylene: Experiment and Theory. *J. Phys. Chem. A* **2001**, *105*, 6655−6667.

(5) Janssens, T. V. W.; Zaera, F. Chemistry of Ethylidene Moieties on Platinum Surfaces: 1,1-Diiodoethane on Pt(111). *J. Phys. Chem.* **1996**, *100*, 14118−14129.

(6) Zaera, F.; Bernstein, N. On the Mechanism for the Conversion of Ethylene to Ethylidyne on Metal Surfaces: Vinyl Iodide on Pt(111). *J. Am. Chem. Soc.* **1994**, *116*, 4881−4887.

(7) Zaera, F.; French, C. R. Mechanistic Changes in the Conversion of Ethylene to Ethylidyne on Transition Metals Induced by Changes in Surface Coverages. *J. Am. Chem. Soc.* **1999**, *121*, 2236−2243.

(8) Azad, S.; Kaltchev, M.; Stacchiola, D.; Wu, G.; Tysoe, W. T. On the Reaction Pathway for the Hydrogenation of Acetylene and Vinylidene on Pd(111). *J. Phys. Chem. B* **2000**, *104*, 3107−3115.

(9) Akita, M.; Hiramoto, S.; Osaka, N.; Itoh, K. Adsorption Structures of Ethylene on Ag(110) and Atomic Oxygen Precovered Ag(110) Surfaces: Infrared Reflection−Absorption and Thermal Desorption Spectroscopic Studies. *J. Phys. Chem. B* **1999**, *103*, 10189−10196.

(10) Merrill, P. B.; Madix, R. J. Hydrogenation of Weakly Rehybridized Ethylene on Fe(100)−H: Ethyl Group Formation. *J. Am. Chem. Soc.* **1996**, *118*, 5062−5067.

(11) Frühberger, B.; Chen, J. G. Reaction of Ethylene with Clean and Carbide-Modified Mo(110): Converting Surface Reactivities of Molybdenum to Pt-Group Metals. *J. Am. Chem. Soc.* **1996**, *118*, 11599−11609.

(12) Böhme, D. K.; Schwarz, H. Gas-phase Catalysis by Atomic and Cluster Metal Ions: The ultimate Single-site Catalysts. *Angew. Chem., Int. Ed.* 2005, 44, 2336−2354.

(13) Yin, S.; Bernstein, E. R. Gas Phase Chemistry of Neutral Metal Clusters: Distribution, Reactivity and Catalysis. *Int. J. Mass Spectrom.* 2012, 321-322, 49−65.

(14) Rao, C. N. R.; Ravenau, B. *Transition Metal Oxides*; CVCH: New York, 1995.

(15) Ioffe, L. M.; Lopez, T.; Borodko, Y. G.; Gomez, R. Oxidative Coupling of Methane Over Natural Manganese Oxide. *J. Mol. Catal. A: Chem.* 1995, 98, 25−34.

(16) Nguyen, K. T.; Zhao, Y. Integrated Graphene/Nanoparticle Hybrids for Biological and Electronic Applications. *Nanoscale* 2014, 6, 6245−6266.

(17) Li, P.; Nan, C.; Wei, Z.; Lu, J.; Peng, Q.; Li, Y. $Mn_3O_4$ Nanocrystals: Facile Synthesis, Controlled Assembly, and Application. *Chem. Mater.* 2010, 22, 4232−4236.

(18) Xiao, J.; Tian, X. M.; Yang, C.; Liu, P.; Luo, N. Q.; Liang, Y.; Li, H. B.; Chen, D. H.; Wang, C. X.; Li, L.; et al. Ultrahigh Relaxivity and Safe Probes of Manganese Oxide Nanoparticles for in Vivo Imaging. *Sci. Rep.* 2013, 3, 3424.

(19) Lee, G. J.; Manivel, A.; Batalova, V.; Mokrousov, G.; Masten, S.; Wu, J. Mesoporous Microsphere of ZnS Photocatalysts Loaded with CuO or $Mn_3O_4$ for the Visible-Light-Assisted Photocatalytic Degradation of Orange II Dye. *Ind. Eng. Chem. Res.* 2013, 52, 11904−11912.

(20) Saravanan, R.; Gupta, V.; Narayanan, V.; Stephen, A. Visible Light Degradation of Textile Effluent Using Novel Catalyst $ZnO/\gamma$-$Mn_2O_3$. *J. Taiwan Inst. Chem. Eng.* 2014, 45, 1910−1917.

(21) Gutsev, G. L.; Rao, B. K.; Jena, P.; Li, X.; Wang, L. S. Experimental and Theoretical Study of The Photoelectron Spectra of $MnO_x^-$ ($x = 1−3$) Clusters. *J. Chem. Phys.* 2000, 113, 1473−1483.

(22) Jia, M. Y.; Xu, B.; Ding, X. L.; He, S. G.; Ge, M. F. Experimental and Theoretical Study of the Reactions between Manganese Oxide Cluster Anions and Hydrogen Sulfide. *J. Phys. Chem. C* 2012, 116, 24184−24192.

(23) Gutsev, G. L.; Rao, B. K.; Jena, P. Photodecomposition of $MnO_4^-$: A Theoretical Study. *J. Phys. Chem. A* 1999, 103, 10819−10824.

(24) Yin, S.; Wang, Z. C.; Bernstein, E. R. O-atom Transport Catalysis by Neutral Manganese Oxide Clusters in The Gas Phase: Reactions with CO, $C_2H_4$, $NO_2$, and $O_2$. *J. Chem. Phys.* 2013, 139, 084307.

(25) Koyama, K.; Kudoh, S.; Miyajima, K.; Mafuné, F. Stable Stoichiometry of Gas-Phase Manganese Oxide Cluster Ions Revealed by Temperature-Programmed Desorption. *J. Phys. Chem. A* 2015, 119, 8433−8442.

(26) Ziemann, P. J.; Castleman, A. W. Mass-spectrometric Investigation of The Stabilities and Structures of Mn-O and Mn-Mg-O Clusters. *Phys. Rev. B: Condens. Matter Mater. Phys.* 1992, 46, 13480−13486.

(27) Kar, P.; Sardar, S.; Ghosh, S.; Parida, M. R.; Liu, B.; Mohammed, O. F.; Lemmens, P.; Pal, S. K. Nano Surface Engineering of $Mn_2O_3$ for Potential Light-harvesting Application. *J. Mater. Chem. C* 2015, 3, 8200−8211.

(28) Ghorai, T. K.; Pramanik, S.; Pramanik, P. Synthesis and Photocatalytic Oxidation of Different Organic Dyes by Using $Mn_2O_3$/$TiO_2$ Solid Solution and Visible light. *Appl. Surf. Sci.* 2009, 255, 9026−9031.

(29) Saravanan, R.; Khan, M. M.; Gupta, V. K.; Mosquera, E.; Gracia, F.; Narayanan, V.; Stephen, A. $ZnO/Ag/Mn_2O_3$ Nanocomposite for Visible Light-induced Industrial Textile Effluent Degradation, Uric Acid and Ascorbic Acid Sensing and Antimicrobial Activity. *RSC Adv.* 2015, 5, 34645−34651.

(30) Popolan, D. M.; Bernhardt, T. M. Interaction of Gold and Silver Cluster Cations with $CH_3Br$: Thermal and Photoinduced Reaction Pathways. *Eur. Phys. J. D* 2011, 63, 251−254.

(31) He, S. G.; Xie, Y.; Guo, Y. Q.; Bernstein, E. R. Formation, Detection, and Stability Studies of Neutral Vanadium Sulfide Clusters. *J. Chem. Phys.* 2007, 126, 194315.

(32) Matsuda, Y.; Bernstein, E. R. On the Titanium Oxide Neutral Cluster Distribution in The Gas Phase: Detection Through 118 nm Single-photon and 193 mn Multiphoton Ionization. *J. Phys. Chem. A* 2005, 109, 314−319.

(33) Matsuda, Y.; Shin, D. N.; Bernstein, E. R. On the Zirconium Oxide Neutral Cluster Distribution in The Gas Phase: Detection through 118 nm Single Photon, and 193 and 355 nm Multiphoton, Ionization. *J. Chem. Phys.* 2004, 120, 4142−4149.

(34) Yin, S.; Bernstein, E. R. Experimental and Theoretical Studies of $H_2O$ Oxidation by Neutral $Ti_2O_{4,5}$ Clusters under Visible Light Irradiation. *Phys. Chem. Chem. Phys.* 2014, 16, 13900−13908.

(35) Yin, S.; Wang, Z. C.; Bernstein, E. R. Formaldehyde and Methanol Formation from Reaction of Carbon Monoxide and Hydrogen on Neutral $Fe_2S_2$ Clusters in The Gas Phase. *Phys. Chem. Chem. Phys.* 2013, 15, 4699−4706.

(36) Yin, S.; Xie, Y.; Bernstein, E. R. Experimental and Theoretical Studies of Ammonia Generation: Reactions of $H_2$ With Neutral Cobalt Nitride Clusters. *J. Chem. Phys.* 2012, 137, 124304.

(37) Yin, S.; Xie, Y.; Bernstein, E. R. Hydrogenation Reactions of Ethylene on Neutral Vanadium Sulfide Clusters: Experimental and Theoretical Studies. *J. Phys. Chem. A* 2011, 115, 10266−10275.

(38) Xue, W.; Wang, Z. C.; He, S. G.; Xie, Y.; Bernstein, E. R. Experimental and Theoretical Study of the Reactions between Small Neutral Iron Oxide Clusters and Carbon Monoxide. *J. Am. Chem. Soc.* 2008, 130, 15879−15888.

(39) Geusic, M. E.; Morse, M. D.; O'Brien, S. C.; Smalley, R. E. Surface Reactions of Metal Clusters I: The Fast Flow Cluster Reactor. *Rev. Sci. Instrum.* 1985, 56, 2123−2130.

(40) Becke, A. D. Density-functional Exchange-energy Approximation with Correct Asymptotic Behavior. *Phys. Rev. A: At., Mol., Opt. Phys.* 1988, 38, 3098−3100.

(41) Becke, A. D. Density-functional Thermochemistry. III. The Role of Exact Exchange. *J. Chem. Phys.* 1993, 98, 5648−5652.

(42) Lee, C. T.; Yang, W. T.; Parr, R. G. Development of The Colle-Salvetti Correlation-energy Formula into A Functional of The Electron Density. *Phys. Rev. B: Condens. Matter Mater. Phys.* 1988, 37, 785−789.

(43) Rassolov, V. A.; Pople, J. A.; Ratner, M. A.; Windus, T. L. 6-31G* Basis Set for Atoms K through Zn. *J. Chem. Phys.* 1998, 109, 1223−1229.

(44) Krishnan, R.; Binkley, J. S.; Seeger, R.; Pople, J. A. Self-consistent Molecular Orbital Methods. XX. A Basis Set for Correlated Wave Functions. *J. Chem. Phys.* 1980, 72, 650−654.

(45) Hehre, W. J.; Ditchfield, R.; Pople, J. A. Self-Consistent Molecular Orbital Methods. XII. Further Extensions of Gaussian-Type Basis Sets for Use in Molecular Orbital Studies of Organic Molecules. *J. Chem. Phys.* 1972, 56, 2257−2261.

(46) Gutsev, G. L.; Rao, B. K.; Jena, P. Systematic Study of Oxo, Peroxo, and Superoxo Isomers of 3d-Metal Dioxides and Their Anions. *J. Phys. Chem. A* 2000, 104, 11961−11971.

(47) Rappe, A. K.; Bernstein, E. R. Ab Initio Calculation of Nonbonded Interactions: Are We There Yet? *J. Phys. Chem. A* 2000, 104, 6117−6128.

(48) Boys, S. F.; Bernardi, F. The Calculation of Small Molecular Interactions by The Differences of Separate Total Energies. Some Procedures with Reduced Errors. *Mol. Phys.* 2002, 100, 65−73.

(49) Li, T. H.; Wang, C. M.; Xie, X. G. C-H Bond Activation of Ethylene by Bare Neutral Palladium and Platinum Atoms: A Theoretical Investigation. *J. Phys. Org. Chem.* 2011, 24, 292−298.

(50) Rivalta, I.; Russo, N.; Sicilia, E. A Theoretical Study of Ethylene Dehydrogenation by Bare Niobium Atom and Cation. *J. Mol. Struct.: THEOCHEM* 2006, 762, 25−31.

(51) Schröder, D.; Shaik, S.; Schwarz, H. Two-State Reactivity as A New Concept in Organometallic Chemistry. *Acc. Chem. Res.* 2000, 33, 139−145.

(52) Kan, C. S.; Su, F.; Calvert, J. G.; Shaw, J. H. Mechanism of The Ozone-ethene Reaction in Dilute $N_2/O_2$ Mixtures Near 1-atm Pressure. *J. Phys. Chem.* **1981**, *85*, 2359−2363.